

RSC Advances



This is an *Accepted Manuscript*, which has been through the Royal Society of Chemistry peer review process and has been accepted for publication.

Accepted Manuscripts are published online shortly after acceptance, before technical editing, formatting and proof reading. Using this free service, authors can make their results available to the community, in citable form, before we publish the edited article. This *Accepted Manuscript* will be replaced by the edited, formatted and paginated article as soon as this is available.

You can find more information about *Accepted Manuscripts* in the [Information for Authors](#).

Please note that technical editing may introduce minor changes to the text and/or graphics, which may alter content. The journal's standard [Terms & Conditions](#) and the [Ethical guidelines](#) still apply. In no event shall the Royal Society of Chemistry be held responsible for any errors or omissions in this *Accepted Manuscript* or any consequences arising from the use of any information it contains.

Continuous-flow droplet-based concentrator using ion concentration polarization

Cite this: DOI: 10.1039/x0xx00000x

Dinh-Tuan Phan,^a Yang Chun,^{*a} and Nam-Trung Nguyen^{*b}

Received 00th March 2015,
Accepted 00th April 2015

DOI: 10.1039/x0xx00000x

www.rsc.org/

We propose a method to continuously generate droplets with programmable concentration using the ion concentration polarization (ICP) phenomenon. The concentration of a sample in continuously formed droplets can be tuned with a combination of flow rate and applied voltage. The nanoporous junction needed for ICP was fabricated by embedding a Nafion membrane inside a PDMS mixture and then self-sealed by curing it. Compared to other methods previously reported in the literature, our fabrication method has the advantages of simplicity, reliability, repeatability and low-cost. Sample droplets with up to 100-fold concentration were generated continuously with our device.

Introduction

Ion concentration polarization (ICP) is a fundamental transport phenomenon that occurs near ion-selective membranes and is often called an ion-depletion and ion-enrichment process¹. Recently, ICP has attracted a great deal of attention from the lab-on-a-chip research community because of its potential applications in biochemical analysis, such as concentration,²⁻⁵ desalination,^{6,7} separation and mixing.^{8,9} Further applications of ICP have been reported recently. Jeon et al.¹⁰ presented a novel separation method, which can continuously separate the particles based on the ICP phenomenon and the electrophoresis mobilities of micro- and nano-sized particles. MacDonald et al.⁷ reported a method of out-of-plane ion concentration polarization for scalable water desalination, which has the advantages of increasing the throughput and the ability of integrating many devices.

A concentrator, that increases the number low-abundant molecules in a given sample volume, is an important tool for biochemical analysis and drug testing. Chen et al.¹¹ introduced an integrated microfluidic device that consists of a biomolecule concentrator and a micro-droplet generator. Concentrating the sample before forming droplets could enhance the limited sensitivity of these droplet-based enzyme assays. However, this device could only generate droplets in an on-demand mode. First, the enzyme molecules were accumulated by a concentrator into a plug, and then, was released by turning off the voltage and transported by pressure-driven flow. Kwak et al.⁵ presented a continuous-flow nanofluidic biomolecule/cell

concentrator, which could accumulate biomolecules and cells into a concentrated plug before the ICP boundary and guided into the narrow, concentrated channel by hydrodynamic force. More recently, Yu et al.¹² reported an on-demand nanofluidic concentrator based on ICP. The device injects concentrated sample in the form of a droplet into an oil stream. The concentration and droplet size depend on the voltage, accumulation time and the period of the injection pulse. A continuous-flow microfluidic device that can both accumulate the low-abundance sample and generate the concentrated droplets at the same time with simple and reliable fabrication process is a critical need for biological applications of microfluidics. In this paper, we first introduce a novel and simple fabrication method to fabricate microfluidic devices with nanoporous materials suitable for establishing ICP. Our method integrates a Nafion membrane into a PDMS layer to form the ion-selective membrane required for ICP. Next, we demonstrate the proof-of-concept of a working concentrator device by continuously generating mono-disperse microdroplets with up to 100-fold concentration of the inlet sample.

Material and methods

Device concept and Fabrication

Our device is a combination of a continuous-flow concentrator⁵ and a droplet generator¹¹ based on the ion concentration polarization. Figure 1 shows the device design and its operation concept. The sample is introduced into the main channel with a

width of 500 μm . At the preconcentrated zone where the sample is concentrated, the inlet channel is bifurcated into a small 50- μm wide concentrating channel and a 450- μm -wide filtering channel. The concentrating channel is slanted 45 degree to allow the stream of concentrated sample to be introduced into the droplet formation part. To establish the preconcentrated zone with ICP, a 50- μm thick Nafion membrane was patterned along the slanted concentrating channel. A buffer channel with 500- μm width and two 8-mm reservoirs form the electric ground for the ICP process. Platinum wires are connected to both sample inlets, and one buffer hole to conduct the electrical current passing through the ion-selective membrane. The filtered, diluted outlet is floated electrically. The gap between buffer channel and main channel is 50 μm . In the droplet formation part, the oil inlet channels have a width of 50 μm . Droplets of the concentrated sample are formed with the flow-focusing configuration. Droplets sample are collected at the 8-mm large outlet reservoirs. The whole system is controlled by the inlet flow rates of the sample inlet and the oil, the applied voltage at the inlet and the outlet pressure. In our later experiments, a voltage ranging between 0 and 150 V was applied between the inlet of the main channel and the buffer channel across the Nafion junction.

Sample flow rates ranging from 10 to 100 $\mu\text{L/h}$ were set by a syringe pump. The outlet pressure is adjusted by the outlet height with a precision lever. On application of an electric field (V^+) across the nanoporous membrane, the ICP zone was developed based on force balance between the depletion force and hydrodynamic force. In Figure 1, the arrows indicate the directions of hydrodynamic force and depletion force acting on charged ions or particles. Depletion force is the force acting on charged species as a result of ICP (ion depletion), which is electrostatic in nature. In the concentrator device, the ICP boundary is generated along the Nafion stripe with a fixed designed distance, and charged species are only accumulated at this zone.

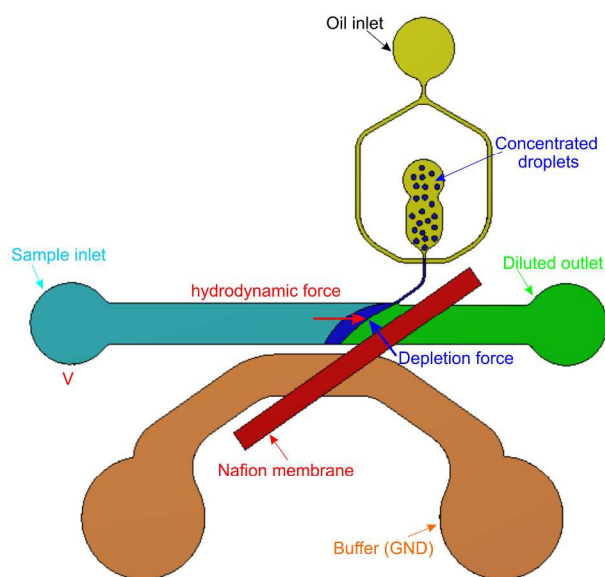


Fig. 1 Working principle of the device

Figure 2 shows the two fabrication processes that can be used to implement the device concept depicted in Fig. 1. Most of the previously reported ICP-based devices used Nafion solution to deposit a thin nanoporous membrane with a thickness varying from 191 nm using micro flow patterning method² to 125 - 200 μm by filling a laser-cut micro channel⁷. To simplify the fabrication process, we used an off-the-shelf Nafion membrane (NR-212, DuPont Co.) with a thickness of 50 μm instead of using the Nafion solution to deposit a thin cation-selective membrane on a glass substrate. This off-the-shelf membrane provides a better mechanical durability and longer working time thus more efficient. Moreover, a thicker membrane generates a stronger electrical repulsive force around the membrane⁴. The silicon wafer was silanized before placing the Nafion membrane, in order to ensure that the Nafion membrane does not stick on the master mould surface when peeling off the PDMS. The microchannels of the device were fabricated following a general PDMS chip fabrication process. The master mold was made with SU-8 photoresist (MicroChem Corp.) and standard photolithography process.

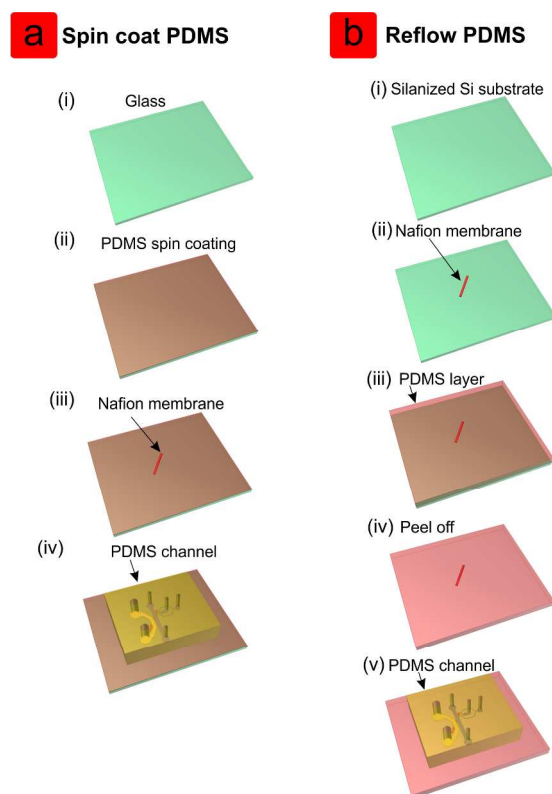


Fig. 2 Fabrication steps for integrating the nanoporous membrane on the device. (a) Integrating a 50- μm thick Nafion membrane on a PDMS/glass substrate. (i) Prepare and clean a glass slide. (ii) Coating the PDMS mixture with a spin speed of 1450 rpm. (iii) Cutting the Nafion membrane and place carefully on top of the PDMS surface. (iv) Bonding the top PDMS with microchannel network to the PDMS/glass substrate with the Nafion membrane using a precision alignment system. (b) Integrating the Nafion membrane on a PDMS-only substrate. (i) Silanizing the silicon substrate. (ii) Cutting the Nafion membrane precisely and stick it on the silanized Si substrate. (iii) Pouring 10 mL PDMS on top of the substrate to an estimated thickness of 1 - 1.5 mm. Reflow at room temperature overnight and then curing at 80°C for 2 hours. (iv) Peeling off the PDMS layer gently. (v)

Bonding the top PDMS with microchannels to the PDMS substrate with Nafion membrane.

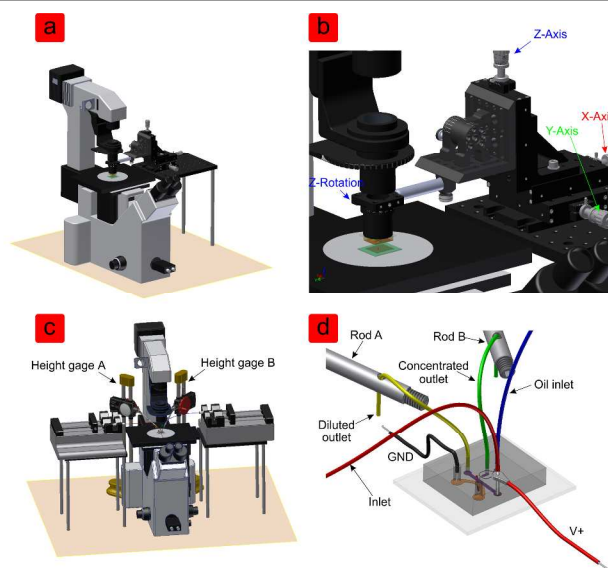


Fig. 3 Experimental setup. (a) The alignment system mounted next to the microscope. All the standard components were from Thorlab. The whole system has the estimated alignment error would be below $1\ \mu\text{m}$. (b) Closer view of the alignment equipment with 4 degrees of freedom. Three transition movements X, Y, Z and one rotation movement around Z axis used to position the top PDMS channel and the bottom glass substrate in place precisely. (c) The experimental setup with syringe pumps and the dial height gages used to control the outlets pressure difference. (d) Tubings and electrical connections of device. The inlet tubing (in red) was connected to $V+$, whereas the buffer channel (in orange) was connected to GND (in black). The diluted outlet (in yellow) and concentrated droplets outlet (in green) were fixed on two rods A, B which were controlled vertically by two dial height gages A and B. The oil inlet was in blue.

Sylgard 184 and a curing agent (Dow Corning Inc.) were mixed in a 10:1 ratio by weight. The mixture was degassed for 1 hour in a vacuum chamber. After that, the mixture was poured onto the silicon master and cured at 80°C for 2 hours. Then the PDMS was peeled off from the SU-8 mold and bonded to the PDMS-glass (Figure 2 (a)) or PDMS-only (Figure 2 (b)) substrate integrated a Nafion membrane with the help of oxygen plasma treatment and under a precise alignment system, Figure 3 (a,b).

As shown in Fig. 2, the device can be fabricated with a glass support or directly on a PDMS substrate. The advantage of the first case is the rigid support of the glass substrate. Figures 4 (a) and (b) shows the layers of the device with glass support and the final device, respectively. To make sure that a thin PDMS is coated, the PDMS mixture can be spin coated before curing in an oven. Figures 4 (c) shows the height if the Nafion membrane relative to the PDMS surface.

Experimental setup

In our experiment, all liquids were kept in 1-ml glass syringes, which were driven by syringe pumps (neMESYS, Cetoni) to deliver the required flow rates to the device. A high-speed CMOS camera (Phantom Miro eX4) attached to a microscope was used to capture the grayscale images. To demonstrate the sample concentration and droplet generation, $1\ \mu\text{M}$ fluorescein

sodium salt (Sigma Aldrich, St. Louis, USA) was used as the inlet sample. We also prepared another concentration of sample $100\ \mu\text{M}$ to measure the reference fluorescence intensity value.

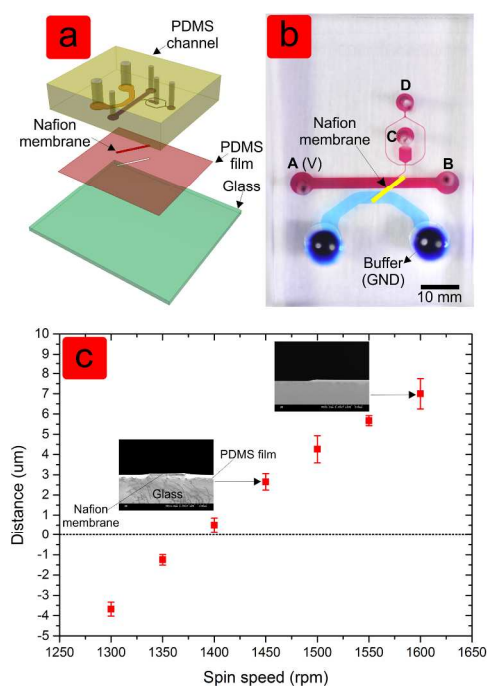


Fig. 4 The structure of device. (b) Fabricated device filled with food dyes. The Nafion membrane (yellow) was patterned in a straight line parallel to the concentrated channel. Red channels were inlet (A) connected to $V+$, diluted outlet (B), concentrated droplets outlet (C) and oil inlet (D). The blue channel was the buffer solution PBS connected to GND. The slanted Nafion membrane was embedded on PDMS layer and aligned during bonding. (c) The relative height between Nafion surface vs PDMS surface coated by varying different spin speeds. Inset are SEM images showing the cross sectional view of a Nafion membrane integrated on a glass substrate coated with PDMS.

Mineral oil (330760, Sigma Aldrich, St. Louis, USA) mixed with 0.5% wt. surfactant Span 80 (S6760, Sigma Aldrich)¹³ work as the the continuous phase for droplet formation. The phosphate buffer solution (PBS) with the concentration of $100\ \mu\text{M}$ was prepared for the buffer channel with the electrical ground.

Platinum wires (Sigma-Aldrich, 0.1-mm diameter) were used as electrodes. The electric fields were provided by a high voltage DC power supply (Model PS350, Stanford Research System, Inc). After recording the images with the high-speed camera, we measured the droplet diameter using a customized MATLAB program. For each data point, a total of 20 droplets were measured. However, as the resultant droplet has an apparent diameter bigger than the depth of the channel, it assumes a discoid shape¹⁴. Hence, the measured result slightly overestimates the actual droplet diameter. The fluorescence intensity of the formed droplet and the distance measurement were processed using another customized MATLAB program.

It is important to control the overall reference pressure of the channels system. To control the effect of the back pressure, the outlets pressure of both concentrated outlet and diluted outlet were compensated using a precision z-movement system. Each opening end of outlet tubing was attached to a dial height

gage (Series 192 with Digital Counter, Mitutoyo, Japan). During the experiment, one can adjust the pressure difference between two outlets to compensate the backpressure effect.

Results and discussions

Concentration with ICP

We characterize the fluorescence intensity at the area located in front of the Nafion membrane to demonstrate the continuous concentration of the device. Once the ICP triggered, all the charged ions will be repelled away from the Nafion membrane and formed a boundary to prevent any charged species to enter this region. The concentration of the fluorescein salt was calibrated against its concentration. The relative intensity ratio between the concentrated sample and the inlet sample of 1 μM allowed the concentration to be determined. Figure 5 shows a representative result of the sample concentration. At 10 $\mu\text{L/h}$ and 30 V a 100-fold concentration from 1 μM to 100 μM can be achieved.

We first fixed the input flow rate and varied the applied voltage to understand the interaction between the hydrodynamic force and the depletion force and the associated location of the preconcentrated zone. Once the ICP is triggered, an preconcentrated zone will appear and stabilise based on the balance between the hydrodynamic force and depletion force. A high applied voltage shifts the preconcentrated zone further away from the Nafion membrane, because the depletion force overcomes the hydrodynamic force and pushes the charged ions away from the nanoporous membrane.

Figure 6 shows the measured distance between the ICP boundary and the edge of the Nafion membrane. In this range, the distance is almost linear to the applied voltage. However, we observed that the ICP boundary fluctuated significantly and may disappear if the applied voltage is too high. These effects could presumably be explained by the breakdown of the PDMS substrate under the threshold voltage. In this situation, short circuit occurred and caused the significant increase in the current, which was monitored continuously by an ampmeter (Keithley). In our experiments, the current was limited to 1 μA by the DC power supply. Therefore, the applied voltage can only be varied in a limited range.

concentrated flow (red line, B), concentrated plug (the peak of the blue line, A) and sample flow (green line, C) are well-defined. The positions of these three lines are located as shown in the inset image. The diluted flow profile can be considered as the later part of the blue curve, which has lower concentration than the sample flow. Fluorescence intensity of the concentrated flow jumped from 20 to 60 (corresponding 1 μM and 100 μM , respectively).

More details are shown in the ESI (details in S1-video, recorded at a rate of 30 frames per second). After the initial test to establish the operation point (10 $\mu\text{L/h}$, 30 V) where the preconcentrated zone is shifted exactly to the concentrating inlet of the droplet formation part, the flow rates were varied from 10 to 50 $\mu\text{L/h}$ to tune the concentration. The concentration at the preconcentrated zone depends on the mass transport of the ions or the supply flow rate at the inlet and the time they are allowed to accumulate. Increasing the inlet flow rate requires a larger voltage to maintain the position of the ICP boundary. In our device, the applied voltage should fall in the range from 10 V to 100 V with a flow rate ranging from 10 to 30 $\mu\text{L/h}$. Figure 6 (b) shows the operation line of our device. Since the applied voltage vary linearly with the inlet flow rate, flow rates used in the experiments of 10, 15, 20, 25, 30 $\mu\text{L/h}$ correspond to the applied voltages of 30, 45, 60, 75, 90 V, respectively. Comparing with the reference operation point of (10 $\mu\text{L/h}$, 30 V, Fig. 7 (a)), we assign each operation point a gain factor of 1, 1.5, 2, 2.5 and 3.

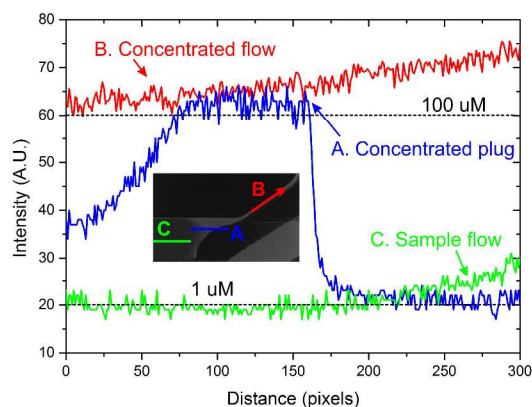


Fig. 5 The fluorescence intensity curve shows a 100-fold jump in the concentration of fluorescein sodium salt at the preconcentrated zone. Flow rate and applied voltage were 10 $\mu\text{L/h}$ and 30 V, respectively. Generation of

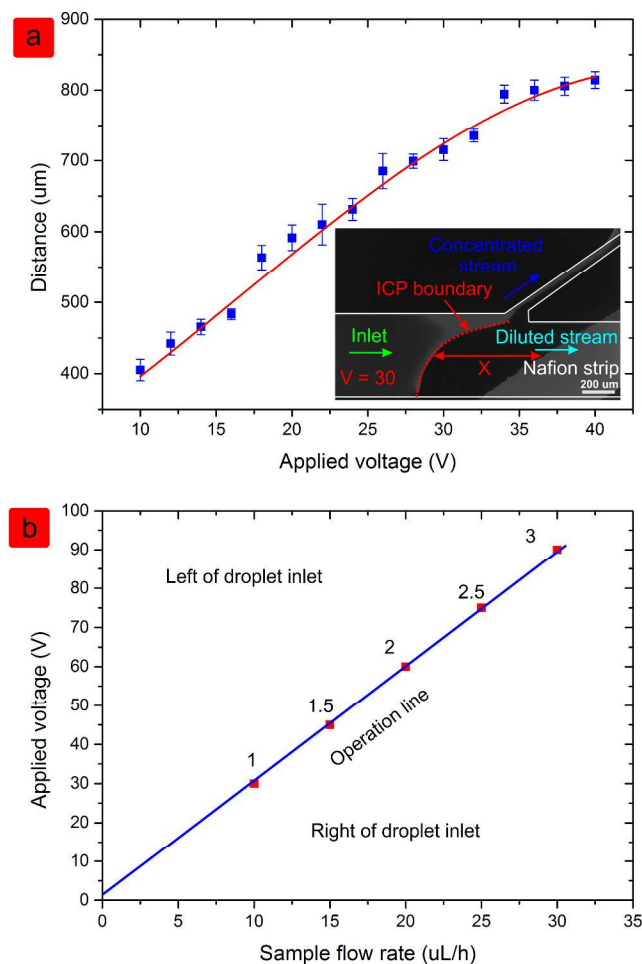


Fig. 6 Controlling the position of the ICP boundary: (a) Effect of the applied voltage under a fix input flow rate of 10 $\mu\text{L/h}$. Inset image shows the distance (denoted in X) measured from the Nafion membrane edge to the outermost of the ICP boundary; (b) The operation line of our device.

At a constant oil flow rate, the size of the formed droplets depends on the inlet sample flow rate. Figure 7 shows the representative droplet formation process at different flow rates and applied voltages. At the reference operation point $Q = 10 \mu\text{L/h}$, $V = 30 \text{ V}$, the ICP boundary is located at the inlet of the droplet formation part, Fig. 7 (a). With an oil flow rate of $Q_{\text{oil}} = 2 \mu\text{L/h}$, stable droplets with concentrated sample are formed, Fig. 7 (b). At a gain factor of 2, the flow rate and the voltage increase to $Q_{\text{in}} = 20 \mu\text{L/h}$ and $V = 60 \text{ V}$, respectively. Since both hydrodynamic force and depletion force increase, the ICP boundary remains at the same position. The inlet flow rate for droplet formation also increases while the oil flow rate remains at $Q_{\text{oil}} = 2 \mu\text{L/h}$, resulting a larger droplet, Fig. 7 (c). At again factor of 3 ($Q_{\text{in}} = 30 \mu\text{L/h}$, $V = 90 \text{ V}$) the formed droplets become even larger, Fig. 7 (d). Figure 8 shows the measured droplet diameter as function of the gain factor.

A higher sample inlet flow rate supplied more charged ions that are accumulated at the ICP boundary and transferred to the droplets. Thus, a higher inlet flow rate or a higher gain factor leads to a higher concentration in the formed droplet. Figure 8 shows that the concentration jumps to more than 100-fold at the gain factor of 2.5, corresponding to the flow rate of 25 $\mu\text{L/h}$ and the applied voltage of 75 V. Increasing the gain factor further, the fluorescence intensity increases slowly and may reach a plateau. This behaviour may be caused by the saturation of the fluorescent intensity.

Conclusion

We demonstrated a continuous droplet-based generator based on the phenomenon of ion concentration polarization. This device can both concentrate and generate the droplets continuously and controllably. The sample can be concentrated by 100-fold with droplet size changing from 25 - 50 μm . The fabrication process for making this device is relatively simple. The use of off-the-shelf Nafion membrane leads to a better durability and a longer lifetime of the device. This concept can be applied for assays with low-abundant input analytes.

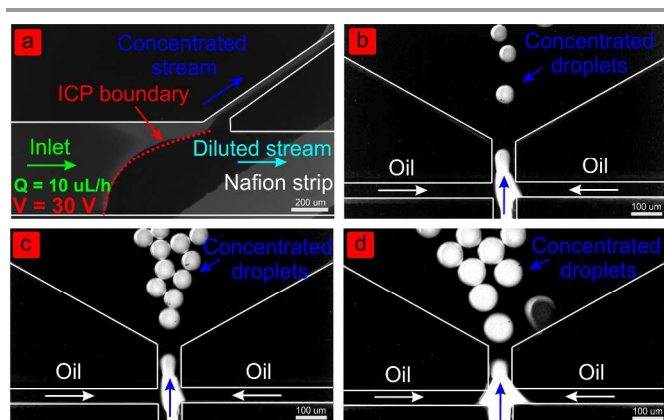


Fig. 7 Droplet generations at different input flow rates and applied voltages: (a) The ICP boundary at $Q_{\text{in}} = 10 \mu\text{L/h}$, $V = 30 \text{ V}$. (b) Droplet formation with $Q_{\text{oil}} = 2 \mu\text{L/h}$, $Q_{\text{in}} = 10 \mu\text{L/h}$, $V = 30 \text{ V}$; (c) Droplet formation with $Q_{\text{oil}} = 2 \mu\text{L/h}$, $Q_{\text{in}} = 20 \mu\text{L/h}$, $V = 60 \text{ V}$; (d) Droplet formation with $Q_{\text{oil}} = 2 \mu\text{L/h}$, $Q_{\text{in}} = 30 \mu\text{L/h}$, $V = 90 \text{ V}$.

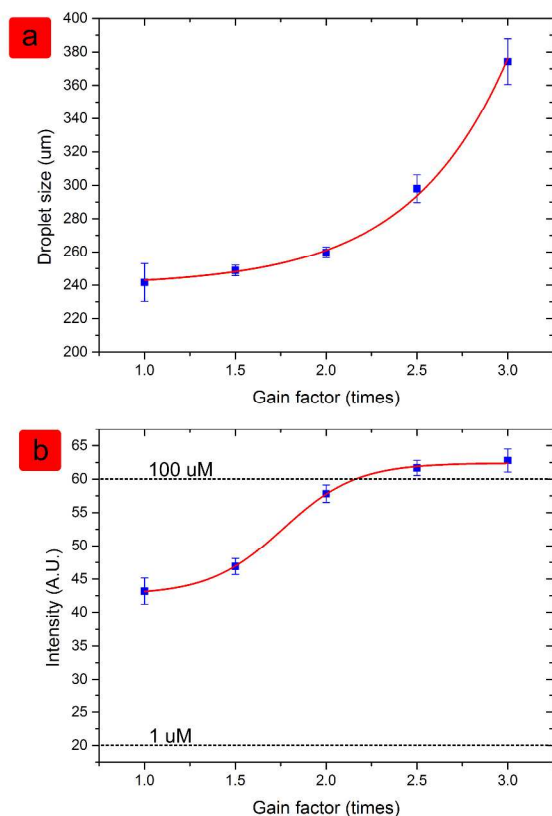


Fig. 8 (a) Relationship between droplets size and the gain factor at a constant oil flow rate of $Q_{oil} = 2 \mu\text{L/h}$. (b) Relationship between the droplet fluorescence intensity and the gain factor. The input sample concentration was $1 \mu\text{M}$ that corresponds to a fluorescence intensity of 20 A.U.

The target analytes can be concentrated to a desired concentration for the subsequent analysis processes.

Acknowledgements

D.T.P acknowledges the support from the PhD Nanyang Research Scholarship (via NEWRI).

Notes and references

^a School of Mechanical and Aerospace Engineering, Nanyang Technological University, 50 Nanyang Avenue, Singapore 639798. Email: MCYANG@ntu.edu.sg

^b Queensland Micro- and Nanotechnology Centre, Griffith University, Brisbane, 4111, Australia. E-mail: nam-trung.nguyen@griffith.edu.au

† Footnotes should appear here. These might include comments relevant to but not central to the matter under discussion, limited experimental and spectral data, and crystallographic data.

Electronic Supplementary Information (ESI) available: movie S1 and movie S2. See DOI: 10.1039/b000000x/

1. Q. Pu, J. Yun, H. Temkin and S. Liu, *Nano Letters*, 2004, 4, 1099–1103.
2. S. J. Kim, Y.-A. A. Song and J. Han, *Chemical Society Reviews*, 2010, 39, 912–22.
3. S. H. Ko, S. J. Kim, L. F. Cheow, L. D. Li, K. H. Kang and J. Han, *Lab on a Chip*, 2011, 11, 1351–1358.

4. S. H. Ko, Y.-A. Song, S. J. Kim, M. Kim, J. Han and K. H. Kang, *Lab on a Chip*, 2012, 12, 4472–82.
5. R. Kwak, S. J. Kim and J. Han, *Analytical chemistry*, 2011, 83, 7348–55.
6. S. J. Kim, S. H. Ko, K. H. Kang and J. Han, *Nature Nanotechnology*, 2010, 5, 297–301.
7. B. D. MacDonald, M. M. Gong, P. Zhang and D. Sinton, *Lab on a Chip*, 2014, 14, 681–685.
8. O. J'annig and N.-T. Nguyen, *Microfluidics and Nanofluidics*, 2011, 10, 513–519.
9. D. Kim, A. Raj, L. Zhu, R. I. Masel and M. A. Shannon, *Lab on a Chip*, 2008, 8, 625–628.
10. H. Jeon, H. Lee, K. H. Kang and G. Lim, *Sci. Rep.*, 2013, 3, 3483.
11. C.-h. Chen, A. Sarkar, Y.-A. Song, M. A. Miller, S. J. Kim, L. G. Griffith, D. A. Lauffenburger and J. Han, *Journal of the American Chemical Society*, 2011, 133, 10368–71.
12. M. Yu, Y. Hou, H. Zhou and S. Yao, *Lab Chip*, 2015, 15, 1524–1532.
13. J.-C. Baret, *Lab on a Chip*, 2012, 422–433.
14. Z. Nie, M. Seo, S. Xu, P. C. Lewis, M. Mok, E. Kumacheva, G. M. Whitesides, P. Garstecki and H. a. Stone, *Microfluidics and Nanofluidics*, 2008, 5, 585–594.

Graphical abstract

We report the continuous generation of droplets with concentrated samples conditioned ion concentration polarization.

